

Simulation of Explosion Crater of Earth Penetrating Nuclear Bomb Based on Equivalency to TNT Mass

Liangquan Wang*, Deren Kong, Fei Shang and Chunyang Zhang

School of Mechanical Engineering, Nanjing University of Science and Technology, Nanjing - 210 094, China

*E-mail: wlq2223263181@163.com

ABSTRACT

The structure size of the crater formed by the earth-penetrating nuclear bomb explosion is one of the important parameters for evaluating the earth-penetrating nuclear bomb damage power. Obtaining the structure size of the crater formed by the earth-penetrating nuclear bomb explosion with different yields is great significance for the evaluation and design of the nuclear bomb damage power. In this study, considering the contradictory relationship between the structure size of the earth-penetrating nuclear bomb and the structure size of the equivalent TNT mass, we propose to use the equivalent energy mapping method to realize the finite element numerical simulation of the earth-penetrating nuclear bomb exploding into craters analyzed and compared the simulation results with the structure size of the crater formed by the ESS nuclear bomb explosion in the United States. The analysis results show that the error between the simulated crater radius and the real crater radius is 3.26%, and the error between the simulated crater depth and the real crater depth is 28.57 %. It meets the calculation accuracy error range of crater formation from nuclear explosion to chemical explosion. Therefore, this method provides an effective numerical simulation method and a means of obtaining the structural size data of the explosion crater for the earth-penetrating nuclear bomb cratering.

Keywords: Projectile penetration analysis; Equivalent TNT mass; Numerical simulation model of explosive crater formation; Equivalent energy mapping

1. INTRODUCTION

The structure size of the crater formed by the ground drilling nuclear bomb explosion on the target is one of the important parameters for evaluating the destructive power of the ground penetrating nuclear bomb¹⁻³. Due to the limitation of nuclear test in the current international form, it is impossible to carry out the research on crater formation by live bomb explosion, and to accurately analyze and evaluate the damage power of ground-penetrating nuclear bomb explosion. Therefore, the research on the finite element numerical simulation method of ground-penetrating nuclear bomb explosion crater formation can make up for the shortage of the current data of live bomb explosion crater formation, improve the understanding of scientific research and design personnel on the damage power of ground-penetrating nuclear bomb, and provide data support for the accurate evaluation and design of the damage power of ground-penetrating nuclear bomb^{4,6}.

Due to the huge power of nuclear test, high cost, and long duration of the hazard of explosive products, there are few researches on ground-penetrating nuclear bombs at home and abroad. For example, Wang, Y.J., *et al.* carried out the numerical simulation of touchdown explosion in pure soil medium around the shock wave effect of touchdown nuclear explosion⁷. The stress wave propagation process obtained from

the numerical simulation is compared with the empirical study, which verifies the rationality of the numerical simulation method and the accuracy of the parameters of the numerical model. Nie, K.L.,⁸ *et al.* studied the electromagnetic pulse coupling characteristics of a certain type of vehicle around the high-altitude nuclear explosion environment, obtained the relevant laws of the electric field distribution inside the vehicle, and put forward electromagnetic pulse protection suggestions.

Peng, G.L.,⁹ *et al.* proposed a fluid-magnetofluid-particle (PIC) hybrid model to describe the debris clouds motion from high-altitude nuclear explosions. They calculated the debris clouds expansion in the Starfish experiment in the United States, and compared the results with the experimental results and verify the solution scheme reliability. Aiming at the multi-field coupling effects problems, geotechnical media strong nonlinearity and large deformation in nuclear explosions, Rong, J.L.,¹⁰ *et al.* proposed an nuclear explosion accurate description method on the ground that comprehensively considered the superposition effect of induced shock waves and direct shock waves. The simulation model was developed, and the simulation model was compared with the experimental data, which proved the simulation method correctness.

Deng, G.Q.,¹¹ *et al.* made statistics on the historical nuclear test data in view of the impact of rock and soil water saturation on the nuclear explosion effect of drilling. Taking the stress and particle velocity as the failure criteria respectively, the minimum thickness of safety protection layer is calculated.

Starting from a high-altitude nuclear explosion X-ray point source, Xu, H.,¹² *et al.* calculated the absorption of different energies X-ray photons in the high-altitude atmosphere by using a detailed energy level model, and obtained the X-ray energy spectrum evolution at different transmission distances and X-rays in the atmosphere spatial distribution of energy deposition in the medium. Gao, R.,¹³ *et al.* made a brief analysis on the formation and distribution of sediment particles, the explosion methods influence on them, and the sediment particles replacement. For a ground explosion with ground material mixed into the fireball, the composition of the settled particles is more complex, and there are certain difficulties in research. Ouyang, J.M.,¹⁴ *et al.* combined the electron number density distribution generated by the delayed radiation ionization of high-altitude nuclear explosions and the WKB method of radio waves propagating in the ionosphere, calculated the radio wave absorption characteristics of high altitude nuclear explosion and compared with the “TEAK” test results.

Fan, Q.X.,¹⁵ *et al.* discussed the seismic magnetic effect generation of underground nuclear explosions and the feasibility of magnetic anomaly measurement, proposed a geomagnetic monitoring method, analyzed its characteristics, and discussed some problems to be solved as a verification technology. Xu, M.,¹⁶ *et al.* established a thermal effect model of light radiation acting on objects by finite element analysis means. Taking the steel structure material of the “Mengshi” vehicle as the research object, the heating of the material and the thermal stress and strain caused by the heating were calculated. Based on the analysis of the underground nuclear explosion shock and vibration effect, Xue, Y.L.,¹⁷ *et al.* discussed the simulation method of shock and vibration effect of underground nuclear explosion, and calculated the shock and vibration effect of closed chemical explosion. Ouyang Jian, M.,¹⁸ *et al.* used a numerical simulation program to simulate the ionization and evolution process of X-rays emitted by high-altitude nuclear explosions to the atmosphere at different heights, and gave the spatiotemporal distribution curve of electrons.

According to the basic shell theory of nuclear explosion particle movement and the interaction mechanism between particles and atmosphere, Yang B, *et al.*¹⁹ established a debris cloud movement simulation method under the geomagnetic field and atmosphere action. Parameters such as expansion scale, velocity, pressure and temperature of debris cloud in different directions in the early post-explosion period are given, which are basically consistent with the literature results. It can be seen from the above research that the current research on nuclear bombs mainly focuses on electronic radiation, spatial distribution of electromagnetic waves and thermal damage, while there are few researches on the size of the crater structure formed by the underground nuclear bombs detonation. Therefore, it is very necessary to carry out the research on the size of the crater structure formed by the underground nuclear bombs detonation.

According to the explosion energy equivalence principle, this study equals the explosive power of earth-penetrating nuclear bomb as equivalent TNT mass, and considers the influence of the TNT explosive structure size on the explosion

crater structure in the case of large equivalent, we proposes the equivalent energy mapping finite element numerical simulation method. The finite element numerical simulation analysis of large-yield TNT simulating the crater formed by the earth-penetrating nuclear bomb was realized, and the accuracy of the simulation model was verified by combining the ESS nuclear bomb actual measurement test crater structure data, which proved the feasibility of the above finite element numerical simulation model.

2. EARTH-PENETRATING NUCLEAR BOMB PENETRATION PROCESS NUMERICAL SIMULATION

2.1 Numerical Simulation Model Establishment

This study is based on the structure of the B61-12 earth-penetrating nuclear bomb, which has a total length of 3.6 m, a projectile diameter of 0.34 m and a total projectile mass of 350 kg.

When constructing the finite element numerical simulation model, the nonlinear display explosion dynamics simulation software AUTODYN was selected to carry out the numerical simulation analysis. The software has many excellent solvers including Euler, Lagrange, ALE, SPH, etc., as well as more than 300 commonly used material databases and fully automatic fluid-structure coupling technology. The software is widely used in the research of ballistics, warhead design, armor piercing, detonation, air and underwater explosions, etc. The calculation results have high accuracy, and have a very good reputation in the international military industry.

In this study, tantalum tungsten alloy (TAN/10%W) was selected as the body material of B61-12, with a density of 18,100 kg/m³. In order not to affect the accuracy of numerical simulation results, according to the convergence analysis of mesh structure size in finite element numerical simulation [20], the mesh structure size was set as 0.01m×0.01m×0.01m. The projectile body penetrated the ground vertically, the ground material was soil, the projectile body penetration speed was 1000 m/s, and the ground grid partition size was 0.012m×0.012m×0.012m. The coupling type between B61-12 missile body and ground is set as Lagrange-Lagrange automatic

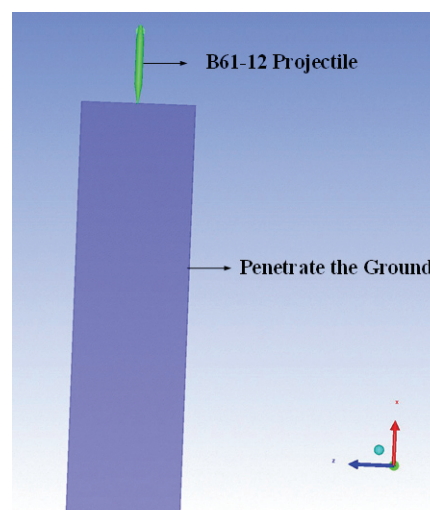


Figure 1. B61-12 earth-penetrating nuclear bomb penetration ground simulation mode.

Table 1. Sandy soil material parameters

$\rho(\text{g} \cdot \text{cm}^{-3})$	G/GPa	B	a_0 / GPa
1.8	6.3×10^{-4}	0.3	3×10^{-13}
C_{vcr_1}	ε^p_1	ε^p_2	ε^p_3
0	0.104	-0.016	-0.192
a_1 / GPa	a_2 / GPa	P_3 / GPa	P_4 / GPa
7.0×10^{-7}	0.30	4.0×10^{-4}	6.0×10^{-3}

coupling. The established finite element numerical simulation model of B61-1 projectile body penetrating the ground is shown in Fig. 1.

In the Fig. 1, the ground material is standard sandy soil, and the sandy soil material parameters are shown in Table 1²¹.

Mohr-Coulomb elastic-ideal plastic model (MC model) is selected to calculate the change rule of sandy soil ground. This model integrates Hooke’s law and Coulomb’s failure criterion, and takes into account the influence of elastic modulus, Poisson’s ratio, effective cohesion, effective internal friction angle and shear expansion angle, so it can well describe the damage phenomenon to sandy soil during projectile penetration and ammunition explosion. MC model is shown in Eqn. (1)²².

$$\tau_n = c_0(1 + \sigma_n / \sigma_t)^{1/m} \tag{1}$$

where, σ_n and τ_n are the shear stress and normal stress at the fracture surface of soil mass respectively; c_0 is the initial cohesion ($c_0 \geq 0$); σ_t is the tensile strength ($\sigma_t \geq 0$); m is the nonlinear coefficient related to soil properties and meets $m \geq 1$.

2.2 Ground-drilling Nuclear Bomb Penetration Simulation Results Analysis

To verify the accuracy of the finite element numerical simulation method of projectile penetrating target, the actual test of steel projectile penetrating concrete target with projectile

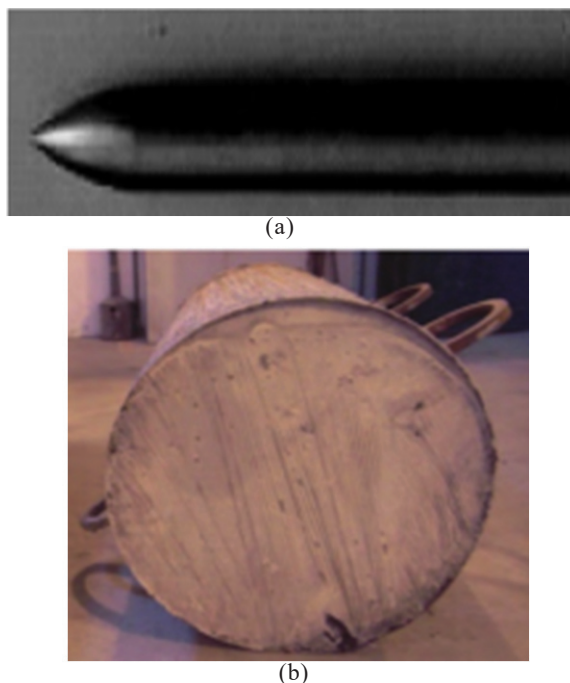


Figure 2. Projectiles and targets physical images: (a) Projectile structure (b) Target structure.

mass of 350 kg and projectile penetrating velocity of 1000 m/s was carried out. The projectile structure and penetration target structure during the test are shown in Fig. 2.

When establishing the finite element numerical simulation model, the main factors affecting the penetration depth of the projectile are the mass of the projectile and the flight speed of the projectile. Therefore, in the actual simulation process, the structural shape of the missile body is simplified, and the simplified missile body model is shown in Fig. 3. The mass of the simplified body is still 350 kg, and the flight speed of the body is 1000 m/s. After the above parameters are set, the finite element numerical simulation analysis of projectile penetrating target can be carried out after the parameters such as calculation times, calculation time, time step and energy overflow are set. After the simulation is completed, the penetration results of the projectile body are analyzed, and the penetration depth of the projectile body to the ground at different penetration times is obtained as shown in Fig. 3. The numerical extraction of the penetration depth of the projectile body is carried out, and the extraction results are shown in Table 2.

From the analysis of Fig. 3 and Table 2, we can find that as the penetration time increases, the projectile penetration

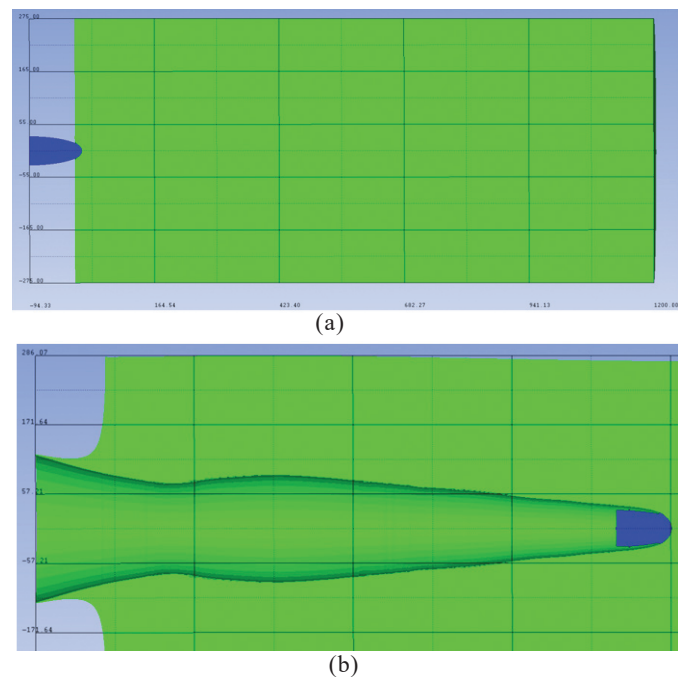


Figure 3. Penetration depth of projectile at different penetration times: (a) Penetration time 0.017 ms (b) Penetration time 1.55 ms.

Table 2 Relationship between projectile penetration time and depth

Penetration time / ms	Penetrate depth / mm
0.017	14.81
0.318	279.86
0.7	545.82
1.047	734.25
1.55	938.21
1.93	938.73
2.12	938.73

depth gradually deepens, the speed of the projectile gradually decreases. When the projectile first touches the ground, the penetration speed is faster. When the projectile penetration speed decreases, the projectile penetration ability gradually weakens until the speed of the projectile decays to 0 m/s. At this time, the projectile remains in the trajectory formed by the penetration process. The change rule between penetration depth and penetration time is shown in Fig. 4.

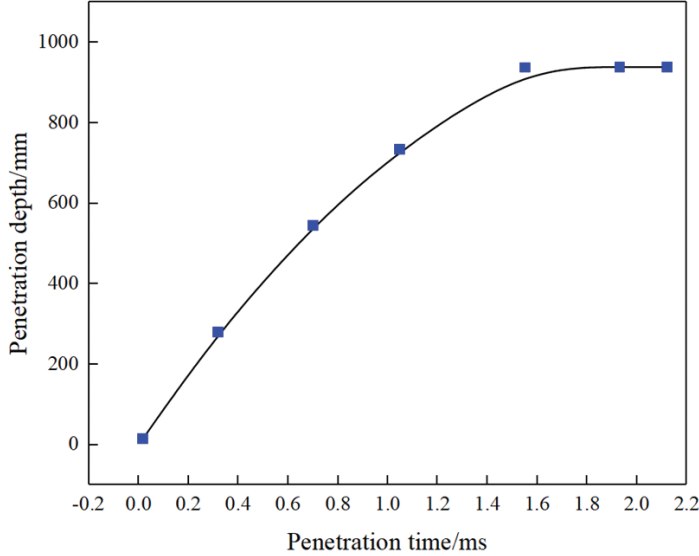


Figure 4. Curve of projectile penetration depth and penetration time.

During the actual test, the projectile penetration concrete targets depth was 795 mm, the depth of finite element numerical simulation penetration targets was 938.21 mm, the difference between the simulation results and the measured penetration depth was 143.21 mm. The relative error rate between the finite element numerical simulation and the measured data is calculated by using the functional relationship shown in Eqn. (2). The calculation result is shown in Eqn. (3), and the relative error rate between the two is 18.08 %. The reason for this error is that the projectile structural shape and the concrete target poured in the actual test process are slightly different from the shape of the simulation model and the selected materials, but it generally conforms to the change rule of the projectile penetration depth in concrete. Therefore, it is feasible to use this method to carry out the finite element numerical simulation calculation of the earth-penetrating nuclear bomb penetration depth.

$$\eta = \frac{H_{\text{Test data}} - H_{\text{Simulation data}}}{H_{\text{Test data}}} \times 100\% \quad (2)$$

$$\eta = \frac{795 - 938.73}{795} \times 100\% = 18.08\% \quad (3)$$

3. FINITE ELEMENT NUMERICAL SIMULATION ANALYSIS OF THE EARTH-PENETRATING NUCLEAR BOMB EXPLOSION INTO A CRATER

3.1 Earth-penetrating Nuclear Bomb is Equivalent to the TNT Mass Model

B61-12 earth-penetrating nuclear bomb equivalent TNT

mass is relatively large, and the common equivalent TNT mass are 0.3 kt, 1.2 kt, 10 kt and 50 kt. The shock wave energy accounts for about 50 % of the total energy during the earth-penetrating nuclear bomb explosion. Therefore, the equivalent TNT mass of the above four equivalent TNT mass converted into the shock wave energy proportion are 0.15 kt, 0.6 kt, 5 kt and 25 kt, respectively. The shape of TNT explosive is a cylinder, and the ratio of height to diameter of the cylinder is 1:1, the equivalent TNT mass structural dimensions are calculated as shown in Table 3.

Table 3. Equivalent TNT mass structure size

Equivalent TNT mass	Charging radius/mm	Charge length/mm
0.15 kt	2446.67	4893.33
0.6 kt	3883.84	7767.68
5 kt	7874.10	15748.20
25 kt	13464.52	26929.04

It can be seen from Table 3 that when the minimum equivalent TNT charge is 0.15 kt, the charge radius reaches 2446.67 mm, the charge length reaches 4893.33 mm, and the size of the charge is larger, while the B61-12 earth-penetrating nuclear bomb diameter is 460 mm. Therefore, if the B61-12 earth-penetrating nuclear bomb is directly detonated by filling with TNT to simulate the cratering process of the B61-12 earth-penetrating nuclear bomb, the structure size of the crater will be affected by the TNT charge structure size, resulting in the cratering results don't conform to the cratering mechanism of the live ammunition explosions. Therefore, it is necessary to design a new method to make TNT explosion craters not affected by the size of the explosive geometry.

To reduce the influence of the structure size of TNT explosive on the explosion crater formation, the finite element numerical simulation model of the pressure propagation distribution of TNT explosive explosion shock wave was established by using the AUTODYN numerical simulation software and the equivalent mapping method of explosion energy. The established model is shown in Fig. 5.

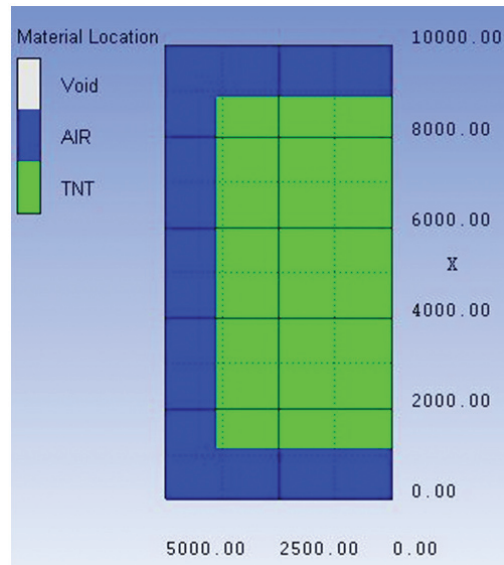


Figure 5. Equivalent TNT explosion finite element numerical simulation model.

In order to use the existing measured data of nuclear bomb explosion to verify the above model accuracy, in the model establishment process, the equivalent TNT mass is 0.6 kt, the density of TNT explosive is 1630 kg/m³, and the length-diameter ratio of the explosive is 1:1. The explosive radius is 3883.84 mm, and the explosive length is 7767.68 mm. The size of the grid structure is 5 mm × 5 mm, and the detonation method is the central point detonation. TNT explosion process is described by JWL Eqn. of state²³, which is shown in Eqn. (4).

$$P=A\left(1-\frac{\omega}{R_1V}\right)e^{-R_1V}+B\left(1-\frac{\omega}{R_2V}\right)e^{-R_2V}+\frac{\omega}{V}E \quad (4)$$

where P is the pressure, V is the volume, E is the internal energy, A and B are the material parameters, R₁, R₂ and ω are constants. The specific values of the parameters are shown in Table 4²⁴⁻²⁵.

Table 4. JWL equation of state parameters

$\rho / (\text{g} \cdot \text{cm}^{-3})$	$D / \text{m} \cdot \text{s}^{-1}$	$P_{\text{cl}} / \text{GPa}$	A / GPa
1.23	4500	5.6	42
B / GPa	R_1	R_2	ω
100	3.55	0.16	0.41

The visible air domain size is 10000 mm × 10000 mm (Length × Width), and the grid structure size is 10 mm × 5 mm. In order to simulate the real environment of the infinite air domain during the actual ammunition explosion, the remaining three sides except the symmetry axis are set as pressure outflow (Flow out), and the ideal gas state Eqn. is used for the air, which is shown in Eqn. (5).

$$P = E \bullet (\gamma - 1) \bullet \rho / \rho_0 \quad (5)$$

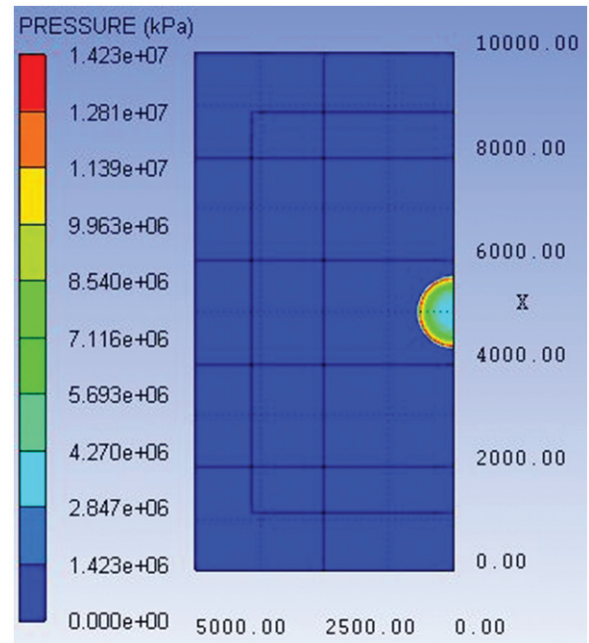
where, P is the gas pressure; γ is the ideal gas constant; ρ is the gas density; ρ₀ is the initial density of the gas; E is the energy density (energy per unit volume of explosive). The air material parameters are shown in the Table 5.

Table 5. Air material parameters

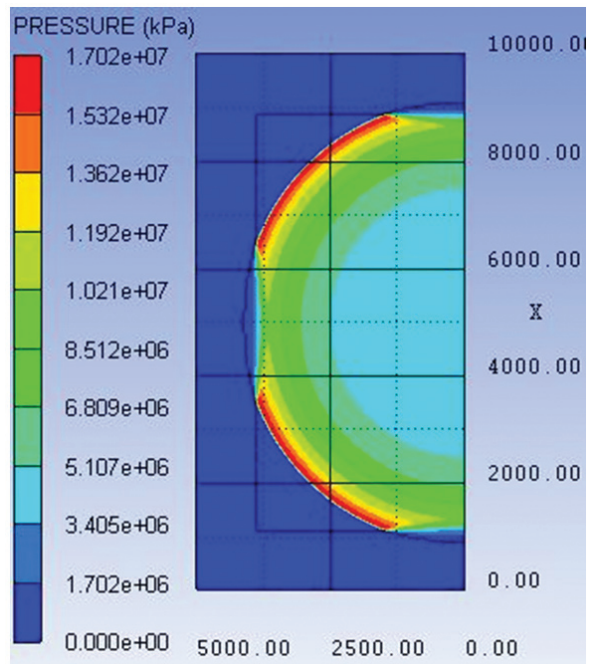
$\rho_0 / \text{kg} \cdot \text{m}^{-3}$	γ	E / MPa
1.225	1.4	0.2533

When the TNT is detonated, the pressure distribution of the shock wave pressure in the air with the explosion time is shown in the Fig. 6.

It can be seen from Fig. 6 that in the early stage of the explosion, with increase of the explosion time, the shock wave propagates outward as a spherical wave, as shown in Fig. 6(a). When the spherical wave propagates to the boundary of the TNT explosive structure, due to the different densities of internal and external interface materials, reflected shock waves will be generated at the interface. The front of the shock wave is affected by the reflected shock wave, resulting in the change of the spherical wave shape, such as shown in Fig. 6(b). At this time, it means that the solid TNT explosive has been completely detonated, and the solid TNT explosive is converted into an explosive product. Use AUTODYN software to output the explosion energy at this moment into a ‘.fil’ format mapping file. The method of energy mapping of blast shock wave is usually used to improve the calculation efficiency and



(a)



(b)

Figure 6. Evolution cloud map of shock wave pressure distribution at different explosion times: (a) Explosion time 0.10 ms (b) Explosion time 0.60 ms.

accuracy of large-scale finite element numerical simulation model. This method has been widely used in the process of pressure propagation of conventional explosive blast wave. For example, in order to simulate the process of underwater explosion shock wave transmission and the first bubble pulsation, Wu, G.M.,²³ *et al.* carried out the three-dimensional model numerical simulation analysis through the energy mapping technology. The numerical simulation results are in good agreement with the empirical formula calculation results. This method greatly improves the calculation efficiency while ensuring the calculation accuracy, and has strong engineering

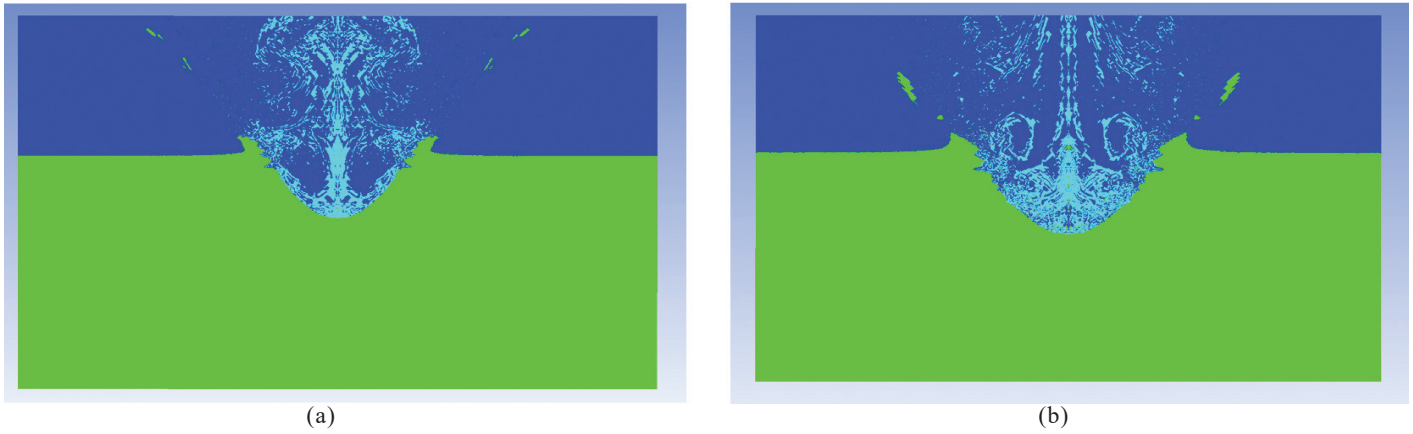


Figure 7. Numerical simulation of crater structure shape: (a) 20 kg TNT explosive (b) 50 kg TNT explosive.

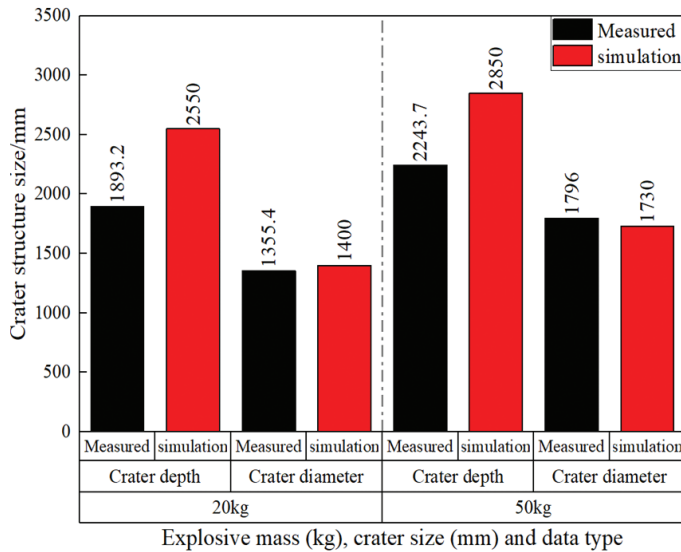


Figure 8. Numerical simulation and actual measurement of crater structure size.

application value. Du, Z.P.,²⁴ *et al.* used the explosion energy mapping technology of the ANSYS-AUTODYN software to carry out the research on the maximum radius and pulsation period of bubbles produced by underwater explosion of the submerged explosive. The theoretical model and the bubble radius, pulsation period and radial motion velocity obtained by simulation are consistent, which shows that this method meets the calculation accuracy requirements required by the project.

To verify the effectiveness of the energy mapping method of explosion shock wave in the process of TNT explosive explosion crater formation, we use the crater data obtained from the explosion test of TNT explosives with mass of 20 kg and 50 kg and buried depth of 0.44 m and 0.60 m in sandy soil to compare with the crater data obtained by the finite element numerical simulation energy mapping method. The crater structure shape, crater diameter and depth data obtained by numerical simulation are shown in Fig. 7 and Fig. 8.

According to the analysis of Fig. 8, the relative errors between the crater diameter and depth formed by the shallow explosion of 20 kg TNT and the measured test results are 3.19 % and 25.76 % respectively; The relative errors between the crater diameter and depth formed by the shallow explosion of 50 kg TNT explosive and the measured test results are 3.81 %

and 21.27 %. The relative error between the results calculated by the finite element numerical simulation energy mapping method and the actual test results meets the requirements of the engineering test accuracy of the explosion field. Therefore, the method of explosion energy mapping can be used to carry out the relevant research when the finite element numerical simulation analysis is carried out for the structure size of the explosion crater of large equivalent TNT explosives.

3.2 Equivalent Energy Mapping Explosion into Crater Structure Size Analysis

When the projectile penetrates the ground at a speed of 0 m/s, the projectile penetration process ends. At the lowest point of penetration trajectory, it is necessary to simulate nuclear bomb explosion and crater formation. Because the projectile speed is 0 m/s at this time, the projectile structure can be deleted, the penetration trajectory left by the projectile penetrating the target can be retained, and the above prepared “. fil” energy mapping file can be imported at the lowest point of the trajectory to map the energy to the coordinate point at the bottom of the trajectory. In this simulation experiment, the buried depth of the reference US ESS nuclear bomb test is 20.4 m, so the coordinates of the energy mapping position are set to (20400,0). Use the “Read Datafile” function in the explosion mechanics simulation software to import the above output shock wave pressure energy mapping file to the mapping coordinate point, and then set the corresponding simulation parameters, such as the number of cycles is set to 1000000, the calculation step is 0.001 ms, the calculation time is 3000 ms, and the maximum energy overflow is set to 999999 (to prevent the numerical simulation from being suspended due to excessive energy overflow). The simulation can be started after the parameters are set. The ground structure will take the mapping coordinate point as the center and explode into craters under the action of the mapping energy. The evolution process of crater structure after explosion energy mapping at different times is shown in Fig. 9.

To quantitatively analyze the size of the crater structure in the explosion energy mapping process, the structure size of the crater under the above seven explosion moments was extracted, and the crater radius and crater depth under different explosion time were obtained as shown in Table 6.

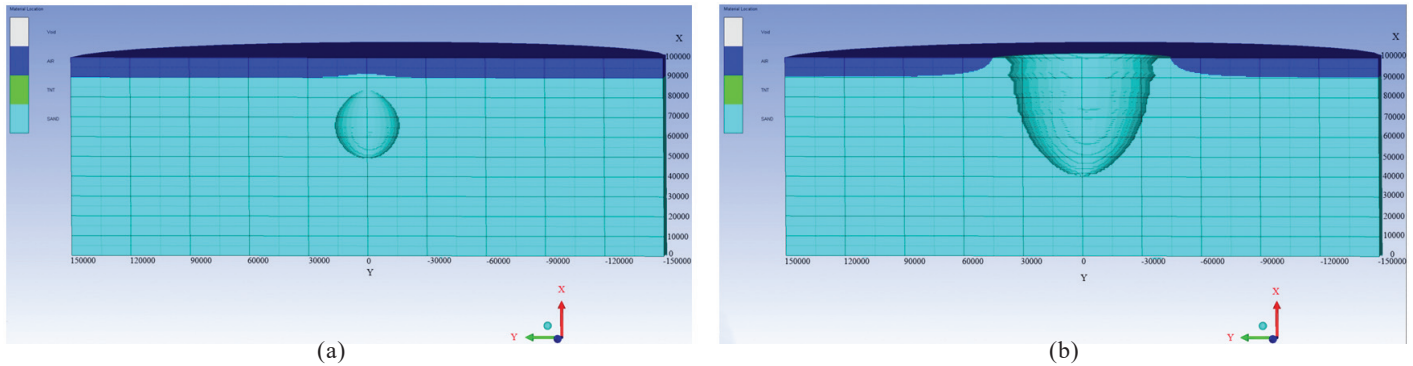


Figure 9. Structure of explosion craters at different explosion times: (a) Explosion time 71.99 ms (b) Explosion time 940.2 ms.

Table 6. Crater structure size detailed parameters at different explosion time

Explosion time /ms	Crater radius / m	Crater depth / m
71.9	--	15.5
166.4	--	44.5
268.7	12.2	46.5
375.7	26.5	48.0
596.3	30.5	49.1
823.8	45.1	49.5
940.2	47.5	49.5

Note: '--' in the above table indicates that the ammunition current explosion has not broken through the ground, and the crater radius has not yet been formed.

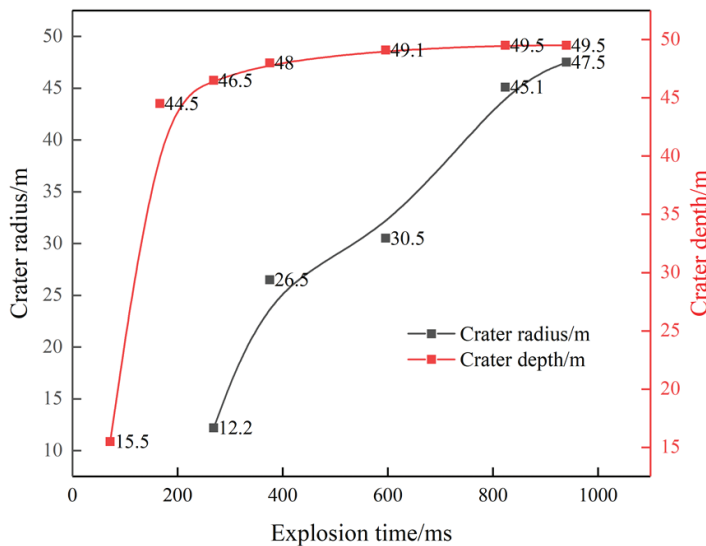


Figure 10. Variation of crater structure size under different explosion times.

To more intuitively and clearly analyze the variation law of the crater radius and crater depth in the explosion energy mapping process, the curves of the crater radius and crater depth at different explosion moments are drawn as shown in Fig. 10.

From analysis of the evolution law of the crater structure size in Fig. 9, Fig. 10 and Table 6, it can be seen that with increase of the explosion time, the crater diameter and depth gradually increase. At the beginning of the explosion, when

the energy generated by the explosion did not break through the sandy soil surface, the high temperature, high pressure gas and the explosion products could not be released, the energy in the internal cavity spread sharply to the surrounding areas, making the crater depth gradually increase. Therefore, in the explosion energy mapping early stage, the energy expansion and evolution is mainly reflected in the increase in the crater depth. However, as the explosive products break through the ground, the high-pressure environment inside the crater is quickly released into the air, lifting the surface of the ground to form an intuitive crater, and the crater diameter gradually increases with the explosion duration. At this time, due to the release of the high-pressure environment to the outside world, the crater internal pressure gradually decreases, so the increase in the crater depth is not obvious, and the crater depth reaches a certain value and does not change. Similarly, when the crater diameter is increased to a certain value, due to the substantial attenuation of the explosion blast wave pressure, it is no longer possible to effectively affect the crater apparent geometry, so even with the explosion time passage, the crater radius no longer changes, that is, the crater maximum radius in Table 6 remains at 47.5 m, and the crater maximum depth remains at 49.5 m.

To verify the accuracy of the above explosion crater finite element simulation model, the simulation data is compared with the measured data of the existing publicly published ESS nuclear bomb explosion crater. The equivalent TNT mass of the ESS nuclear bomb is 600 t, and the explosion apparent crater diameter and depth when the ammunition is buried at a depth of 20.4 m are 46 m and 38.5 m, respectively. Compare the crater structure parameters obtained by the blast energy equivalent mapping method with the ESS nuclear bomb measured data, calculate the relative error between the simulated crater radius and depth and the measured crater radius R and depth H of the ESS nuclear bomb. The functional relationship for calculating the relative error of crater radius is shown in Eqn. (6); The functional relationship for calculating the relative error of crater depth is shown in Eqn. (7).

$$\varphi_R = \frac{R_{\text{Simulation data}} - R_{\text{Test data}}}{R_{\text{Test data}}} \times 100\% \tag{6}$$

$$\phi_H = \frac{L_{\text{Simulation data}} - L_{\text{Test data}}}{L_{\text{Test data}}} \times 100\% \tag{7}$$

Substitute the above finite element numerical simulation

data and measured data into Eqn. (6) and Eqn. (7) to calculate the relative error rate of explosive crater radius as shown in Eqn. (8), and the relative error rate of explosive crater depth as shown in Eqn. (9).

$$\varphi_R = \frac{47.5 - 46}{46} \times 100\% = -3.26\% \quad (8)$$

$$\phi_H = \frac{49.5 - 38.5}{38.5} \times 100\% = 28.57\% \quad (9)$$

As can be seen from the above calculation results, the absolute values of the relative errors between the radius and depth of the crater formed by the finite element numerical simulation and the measured radius and depth of the crater of the ESS nuclear bomb explosion are 3.26 % and 28.57 %, respectively, for 600t equivalent TNT explosive mass and 20.4 m explosive burial depth. It can be concluded that the crater radius obtained by the method of explosion energy equivalent mapping is very close to the measured results, but there is a large error between the explosion crater depth. Analysis the reason is that the sandy soil structure changes with the increase of depth in the actual test, such as the sandy soil contains rocks, gravel and so on, which leads to the change of the sandy soil structure mechanical properties. However, in the process of finite element numerical simulation, the sandy soil structure model is isotropic, and the mechanical properties are stable, so the simulation results have certain error with the measured results, but according to the accuracy requirements of finite element numerical simulation of nuclear detonation transformation explosion in China, the error accuracy between the simulation results and the measured results is less than 30 %. Therefore, the finite element numerical simulation model of explosion cratering established in this study is valid. This method can be applied to the numerical finite element simulation analysis of the ground cratering structure of nuclear explosion transformed into chemical explosion.

4. CONCLUSIONS

In this study, finite element numerical simulation method was used to analyze the target penetration depth and crater structure of a certain type of earth-penetrating nuclear bomb, and the simulation results were compared and verified with the measured data. The verification results show that the finite element numerical simulation analysis is carried out for the penetration depth of a 350 kg earth-penetrating nuclear bomb into concrete target, and the simulation results are in good agreement with the measured results. Using the explosion energy equivalent mapping method proposed in this study, the finite element numerical simulation analysis of the underground explosion crater formation of the ESS nuclear bomb with the equivalent TNT explosive mass of 600 t was carried out, and the simulation calculation accuracy met the accuracy requirements of the nuclear explosion into chemical explosion crater formation. This method has good adaptability to the crater formation of nuclear bomb explosion when the mass of equivalent TNT explosive is large equivalent, and provides an effective numerical simulation method and data acquisition method for the earth-penetrating nuclear bombs explosion crater.

REFERENCES

1. Wang, Z.X. Underground bunker busters: US Army Ground Drill Bomb[J]. *Life and Disaster*, 2012, **02**, 10-11.
2. Ding, Y. & Ding, P. Hard shield against earth penetrating nuclear bombs. *National Defense Sci. Technol.*, 2001, **22** (09), 53-55.
doi: 10.13943/j.issn1671-4547.2001.09.008
3. Qing, J.H. & Wang, L.H. Preliminary analysis of explosion effects of earth penetrating nuclear bombs. *Nuclear Electron. Detection Technol.*, 2006, **04**, 481-485.
4. Kuang, X.H.; Zhu, Q.C. & Zhang, Z.Y. A review of the development of new strategic weapons in the United States. *National Defense Sci. Technol.*, 2008, **01**, 21-32.
5. Deng, C.M.; Xu, J.Y. & Wu, H. Penetration depth and crater effect of B61-11 ground-drilling nuclear bomb. *Acta Projecta Sinica*, 2007, **05**, 116-118.
doi: 10.15892/j.cnki.djzdx.2007.05.026
6. Robert, W.N. Low-yield earth-penetrating nuclear weapons. *Sci. Amp; Global Security*, 2002, **10**(1).
doi: 10.1080/08929880290008386
7. Wang, Y.J.; Yan, F.G.; Chen, J.Y.; Xue, H. & Liang, J. Numerical simulation of shock wave effect of touch-touch nuclear explosion. *Shanxi Architecture*, 2022, **48**(01), 58-63+69.
doi:10.13719/j.cnki.1009-6825.2022.01.018
8. Nie, K.L.; Zhao, W.; Li, P.; Wei, Y.L. & Liu, X. Electromagnetic pulse coupling characteristics of a certain type of vehicle in high-altitude nuclear explosion environment. *J. Ordnance Industry*, 2020, 1-10.
9. Peng, G.L. & Zhang, J.J. Simulation of debris clouds of high-altitude nuclear explosion based on fluid-magnetic fluid-particle mixing method. *Acta. Physica. Sinica.*, 2021, **70**(18), 113-119.
doi:10.7498/aps.70.2.0.210347
10. Rong, J.J.; Song, Y.B.; Wang, X.; Guo, Z. & Xiang, D.L. Equivalent simulation of soil motion characteristics under the impact of nuclear explosion on the ground. *J. Ordnance Eng.*, 2021, **42**(01), 56-64.
doi:10.3969/j.issn.1000-1093.2021.01.006
11. Deng, G.Q.; Gao, W.L.; Xue, Y.L.; Gao, W.L.; Xue, Y.L. & Liu, Y.L. Differential analysis of nuclear explosion effects in dry and wet rocks. *Protection Engineering*, 2020, **42**(01), 24-29.
12. Xu, H.; Ou, J.M.; Wang, S.W.; & Gao, C. Numerical simulation of X-ray energy deposition and fireball radiation process of high-altitude nuclear explosion. China Nuclear Science and Technology Progress Report (Volume 6)-Proceedings of the 2019 Annual Conference of the Chinese Nuclear Society, 2019, **7**, 14-20.
doi:10.26914/c.cnkihy.2019.056413
13. Gao, R. & Wang, B.R. Research on the characteristics of radioactive fallout particles in nuclear explosion. Proceedings of the 19th National Annual Conference on Nuclear Electronics and Nuclear Detection Technology, 2018, 376-381.
doi:10.26914/c.cnkihy.2018.001025
14. Ou, J.M.; Ma, Y.Y.; Shao, F.Q. & Hu, L.X. Study on the

- effect of ionization on radio wave propagation by high-altitude nuclear explosion radiation. Abstracts of the 18th National Plasma Science and Technology Conference, 2017, 189.
15. Fan, Q.X.; Li, T.H.; Zhou, J.D. & Fang, Z. Discussion on the application of seismic effect of underground nuclear explosion in nuclear verification. National Security Geophysics Series (XI)-Frontiers of Geophysical Applications, 2015, 222-224.
 16. Xu, M.; Zhu, J.; Wang, L.H. & Li, X.L. Numerical simulation of the thermal effect of nuclear explosion light radiation on objects. Proceedings of the 17th National Annual Conference on Nuclear Electronics and Nuclear Detection Technology, 2014, 445-448.
 17. Xue, Y.L.; Tang, D.G. & Mo, M.L. Discussion on the method of simulating the shock effect of underground nuclear explosion. Proceedings of the 2013 Annual Work Conference and Academic Exchange Meeting of the Engineering Blasting Professional Committee of the Chinese Mechanics Society, 2013, 70-72+132.
 18. Ou, J.M.; Ma, Y.Y.; Shao, F.Q. & Zou, D.B. Numerical simulation of X-ray ionization and evolutionary process of atmosphere under high-altitude nuclear explosion. *Acta Physica Sinica*, 2012, **61**(08), 135-140.
 19. Yang, B.; Niu, S.L.; Luo, X.D. & Huang, L.X. Numerical simulation of the movement of debris clouds of high-altitude nuclear explosion[J]. *Nuclear Technol.*, 2012, **35**(02), 156-160.
 20. Ma, Y.; He, Y.; Wang, C. Influence of lining materials on the detonation driving of fragments. *J. Mech. Sci. Technol.*, 2022.
doi:10.1007/s12206-022-0223-6.
 21. Wang, L.Q.; Shang, F.; Zhang, J.W. & Wang, R. Experimental study on numerical simulation of damage power of high-energy explosives. *J. Testing Technol.*, 2021, **35**(01), 6-11.
doi:10.3969/j.issn.1671-7449.2021.01.002.
 22. Wang, H.T.; Chen C.Y.; Zhang H.J. & Zhang, X.Q. Prediction method of uplift bearing capacity of shallow-buried inclined strip anchor plate based on nonlinear Mohr-Coulomb failure criterion. *Eng. Sci. Technol.*, 1-11.
doi:10.15961/j.jsuese.202101134
 23. Wang, L.Q.; Shang, F. & Kong, D.R. Numerical simulation analysis of static burst shock wave. *Chinese J. Ordnance Equipment Eng.*, 2020, **41**(12), 208-213.
doi: 10.11809/bqzbgcxb2020.12.039.
 24. Wu, G.M.; Zhou, X.T. & Xiao, H.L. Numerical simulation of underwater explosion. *Ship Sci. Technol.*, 2012, **34**(09), 20-26.
doi:10.3404/j.issn.1672-7649.2012.09.004
 25. Du, Z.P.; Wang, Y. & Xin, C.L. Simplified model and numerical simulation of bubble explosion of underwater rigid wall charge [J]. *Comput. Simulation*, 2009, **26**(04), 10-17
doi:1006-9348(2009)04-0010-04

ACKNOWLEDGMENT

This work is supported by National Defense Basic Scientific Research Project, project numbers JSJL20166060B001D.

CONTRIBUTORS

Dr Lianguan Wang obtained his PhD from Nanjing University of Science and Technology, China. His current research interests are blast field damage measurement testing and evaluation. He is responsible for the writing and revision of this manuscript.

Dr Deren Kong obtained his PhD from Nanjing University of Science and Technology, China. He is working as Professor. His research direction is the modern test measurement theory and application. He is responsible for overall organisation of this manuscript.

Dr Fei Shang obtained his PhD at Jilin University. He is working as a Professor. His research direction is special environmental parameter testing technology and damage power testing and evaluation research. He is responsible for the overall review of this manuscript.

Dr Chunyan Zhang obtained his PhD from Nanjing University of Science and Technology, China. His current research interests are blast field damage measurement testing and evaluation. She is responsible for the overall review of this manuscript.